NASA TECHNICAL
MEMORANDUM

Report No. 53870

A DIRECT MEASUREMENT OF THE MOST PROBABLE PREFERRED ANGULAR VELOCITY OF TURBULENT STRUCTURES BY OPTICAL CORRELATION OF LASER SCHLIEREN SIGNALS

By B. H. Funk
Aero-Astrodynamics Laboratory

August 26, 1969

NASA

George C. Marshall Space Flight Center
Marshall Space Flight Center, Alabama

TECHNICAL REPORT STANDARD TITLE PAGE

1. REPORT NO.	2. GOVERNMENT ACCESSION NO.	3. RECIPIENT'S CATALOG NO.
NASA TM X-53870		

4. TITLE AND SUBTITLE	5. REPORT DATE
A DIRECT MEASUREMENT OF THE MOST PROBABLE PREFERRED ANGULAR VELOCITY OF TURBULENT STRUCTURES BY OPTICAL CORRELATION OF LASER SCHLIEREN SIGNALS	August 26, 1969
	6. PERFORMING ORGANIZATION CODE
7. AUTHOR(S) B. H. Funk	8. PERFORMING ORGANIZATION REPORT #
9. PERFORMING ORGANIZATION NAME AND ADDRESS NASA George C. Marshall Space Flight Center Marshall Space Flight Center, Alabama 35812	10. WORK UNIT NO.
	11. CONTRACT OR GRANT NO.
12. SPONSORING AGENCY NAME AND ADDRESS	13. TYPE OF REPORT & PERIOD COVERED Technical Memorandum
	14. SPONSORING AGENCY CODE

15. SUPPLEMENTARY NOTES

Work performed by Aero-Astrodynamics Laboratory, Science and Engineering Directorate

16. ABSTRACT

A method which potentially provides the means for separating the translational and rotational motion of turbulent structures is introduced. Simple two-dimensional models are used to relate the skewness of cross-correlograms computed from laser schlieren signals to the rotation of flow disturbances. The method, referred to herein as the method of "forced similarity," is discussed with respect to application to the turbulent free shear layer of an axisymmetric supersonic jet. Experimental results show that the shape of the cross-correlogram in the neighborhood of the "peak" is strongly influenced by rotational motion, and therefore, it becomes necessary to account for the effect in order to determine the correct statistical properties of the turbulence.

17. KEY WORDS	18. DISTRIBUTION STATEMENT
	PUBLIC RELEASE: E. D. Geissler Director, Aero-Astrodynamics Laboratory

19. SECURITY CLASSIF. (of this report)	20. SECURITY CLASSIF. (of this page)	21. NO. OF PAGES	22. PRICE
UNCLASSIFIED	UNCLASSIFIED	32	

MSFC - Form 3292 (May 1969)

LIST OF ILLUSTRATIONS

DEFINITION OF SYMBOLS

Symbol	Definition
A	beam A, upstream beam
B	beam B, downstream beam
C	a constant ($C = 4\bar{I}_d/\pi D$)
D	diameter of laser beam; photodetector
$\bar{I}_d$	absolute time averaged current supplied to photodetector with knife-edge removed
$i(t)$	ac-electrical signal output of photodetector
$K(\xi, \psi_a, \psi_b, \psi_c)$	similarity function
$R(\xi, \tau)$	cross-correlation function or cross-correlogram of beam A
s	sensitivity of laser schlieren beam
T	integration time for computation of cross-correlation
t	time
$<U>$	the most probable speed of disturbances averaged over the beam separation distance ξ
x,y,z	coordinates in direction of flow, perpendicular to flow direction (in horizontal plane), and perpendicular to flow direction (in vertical direction), respectively
α	Gladstone-Dale constant
$\underline{\Delta}$	beam deflection vector
ξ	beam separation distance
ρ	air density
τ	time delay of downstream signal
$\emptyset$	angle of rotation of $\underline{\Delta}$ during transit time of disturbance from beam A to B

DEFINITIONS OF SYMBOLS (Cont'd)

Symbol	Definition
θ	angle measured from x-axis to beam deflection vector, $\underline{\Delta}$
$\langle \underline{\omega}_p \rangle$	the most probable preferred angular velocity of the disturbances
$( )'$	fluctuating component
$\overline{( )}$	time average
$\underline{( )}$	vector
$(\hat{})$	unit vector
$\langle \rangle$	expectation value, or most probable value

Subscripts

x,y,z	component in direction of x,y,z-axis, respectively
a,b	beam A,B
c	refers to angle between beam B and the Z-axis
1,2	case A, no rotation; case B, rotation
m	most probable; maximum

TECHNICAL MEMORANDUM X-53870

A DIRECT MEASUREMENT OF THE MOST PROBABLE PREFERRED ANGULAR VELOCITY OF TURBULENT STRUCTURES BY OPTICAL CORRELATION OF LASER SCHLIEREN SIGNALS

SUMMARY

A method is introduced which provides the means for separating the translational and rotational motion of turbulent structures. Simple two-dimensional models are used to relate the skewness of cross-correlograms computed from laser schlieren signals to the rotation of flow disturbances. The method, referred to herein as the method of "forced similarity," is discussed with respect to application to the turbulent free shear layer of an axisymmetric supersonic jet. Experimental results show that the shape of the cross-correlogram in the neighborhood of the "peak" is strongly influenced by rotational motion, and therefore, it becomes necessary to account for the effect in order to determine the correct statistical properties of the turbulence.

I. INTRODUCTION

This document contains the author's preliminary thoughts on the possibility of making direct measurements of the most probable preferred angular velocity at "localized" regions within turbulent flows by optical correlation of laser schlieren signals [2]. Although some experimental results are presented which satisfy certain necessary conditions required of the proposed theory, sufficient data verifying the theory do not presently exist. However, plans have been made to obtain these data in Marshall Space Flight Center's Cold Flow Thermal and Acoustic Jet Facility.

During the feasibility test presented in reference 2, there were unexplained variations in the shape of the cross-correlograms computed from laser schlieren signals retrieved from the supersonic turbulent boundary layer on a thin plate. In April 1968, near the conclusion of this test, the connection between the skewness of the cross-correlograms and the angular rotation of the disturbances was considered.

Preliminary experimental results eventually led to a method for separating rotational and translational contributions to the computed cross-correlograms. This method is referred to herein as the method of "forced similarity." The "forced similarity" condition provides the means for direct measurement of the most probable preferred[1] angular velocity of the turbulent structures[2] at localized regions inside turbulent flows. The potential extension of the method to yield the probability distribution of the angular velocity and measurements of vorticity are very interesting, and may result as a natural consequence of the development of the laser schlieren system.

II. THE LASER SCHLIEREN OPTICAL REMOTE SENSING SYSTEM

For simplicity, let us consider the model of a laser schlieren optical remote sensing system shown in figure 1[3] where two laser beams of light are directed through the test section of a wind tunnel. The parallel beams are perpendicular to the flow and separated by a distance ξ. The plane formed by the beams is such that flow disturbances passing through the upstream beam (beam A) at time t, also pass through the downstream beam (beam B) at a later time $t + \tau$. A knife-edge is positioned perpendicular to each of the beams such that 50 percent of the light is prevented from reaching the respective photodetectors when the beams are undisturbed.

Reference 2 shows that a disturbance characterized by a local gradient of the index of refraction will deflect each of these beams as it passes through them. Each deflection is proportional to the component of the gradient which is perpendicular to the path of the beam. When a deflection occurs, the amount of light reaching the photodetector is changed. The photodetector converts this change into an ac-electrical

---

[1]The word "preferred" is used since the statistical process does not yield the angular velocity components based upon statistical averages of absolute values.

[2]Throughout this report reference is made to "turbulent structures" and "disturbances" in order to distinguish between the motion of the density gradient and the motion of fluid particles which represent an "eddy" at a particular instant. The laser schlieren signals are produced by the fluctuating density gradient component perpendicular to the path of the beam [3].

[3]This system is described in detail in reference 2.

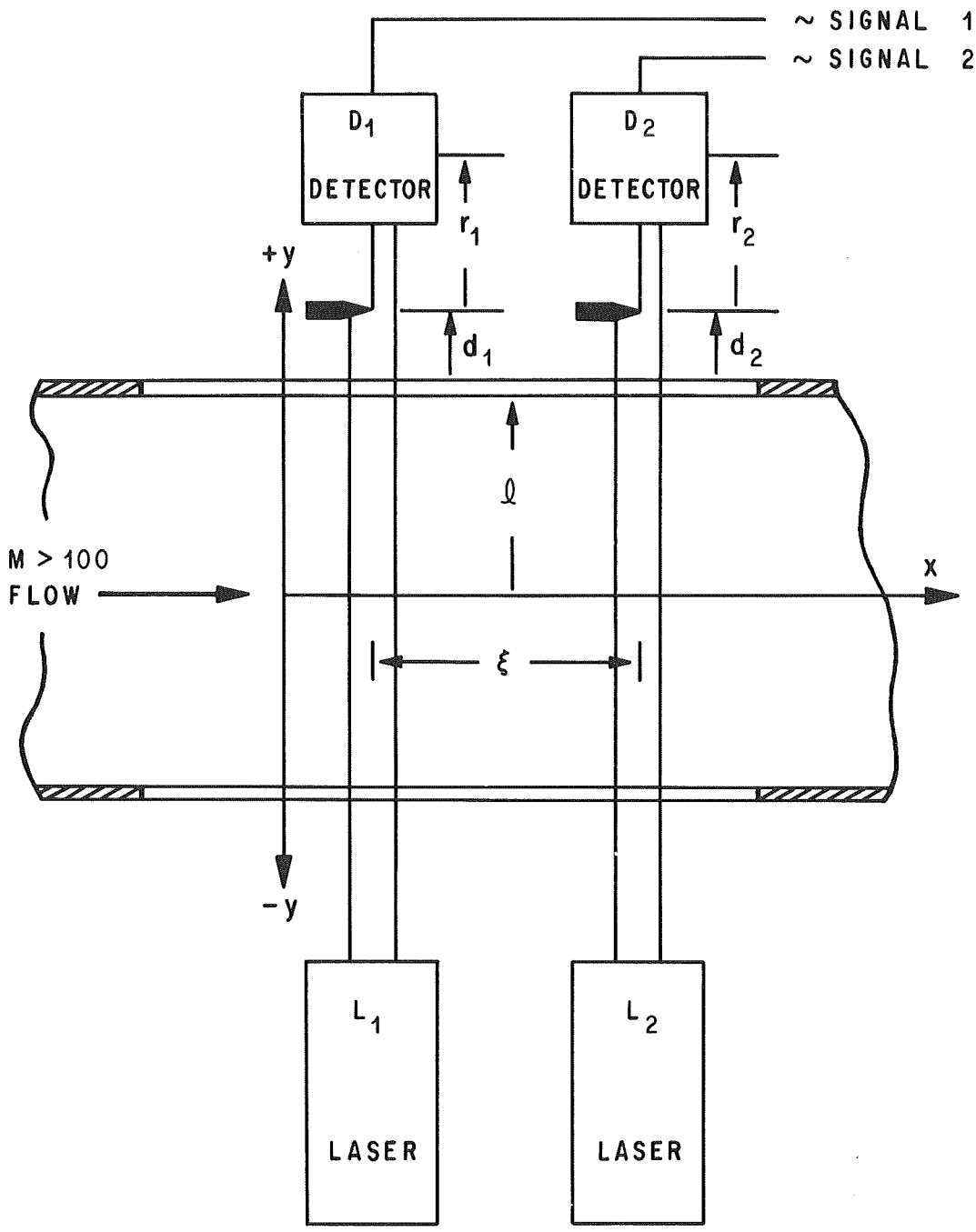

Figure 1. A Schematic of A Laser Schlieren System Using Parallel Beams

signal. Therefore, the output signal of the photodetector is related to the beam deflection which is caused by a local gradient characterizing a particular flow disturbance passing through the laser beam.

Because the refractive index of air is proportional to the density (to a good approximation), the output signal of the photodetector is proportional to the change in the component of the density gradient which is perpendicular to the beam and to the knife-edge.

$$i(t) \doteq \alpha \left[s \frac{\partial \rho'(t)}{\partial x} \right]_{avg.} \cdot \qquad (1)$$

In equation (1), s is the sensitivity of the beam, α is the Gladstone-Dale constant [3], and i(t) is the output signal of the photodetector. Also, the knife-edge was assumed to be perpendicular to the x-direction as shown in figure 2.

Figure 2, a view taken along the centerline of the laser beam (either beam A or B) from laser toward detector, shows the knife-edge, the eye of the photodiode, and the laser beam cross section. The beam is shown in the undisturbed position and in a deflected position described by the beam deflection vector, $\underline{\Delta}$.

In the following let $\Delta(t)$ and $\theta(t)$ represent the magnitude and direction of $\underline{\Delta}(t)$, respectively. Further, assume that the eye of the photodiode has a large area of constant sensitivity compared to the cross sectional area of the laser beam, and that no laser light falls outside of this area of constant sensitivity. If the intensity across the laser beam is assumed to be constant over the beam cross-section and that the knife-edge is straight, the relationship between the time histories of the beam deflection vector and the photodetector ac-electrical output is simplified considerably.

Because the area of sensitivity of the eye of the photodiode monitoring the fluctuating laser light is constant, the component of the beam deflection vector which is parallel to the knife-edge does not contribute to the output signal of the photodetector. The component of $\underline{\Delta}$ which is perpendicular to the knife-edge will determine the amount of change in light reaching the photodiode. If the beam deflection is small compared to the diameter of the laser beam, the output signal, i(t), can be expressed conveniently as a function of the component $\underline{\Delta}$ which is perpendicular to the knife-edge:

$$i(t) = \left[\frac{4\bar{I}_d}{\pi D} \right] \Delta_x(t) \qquad (2)$$

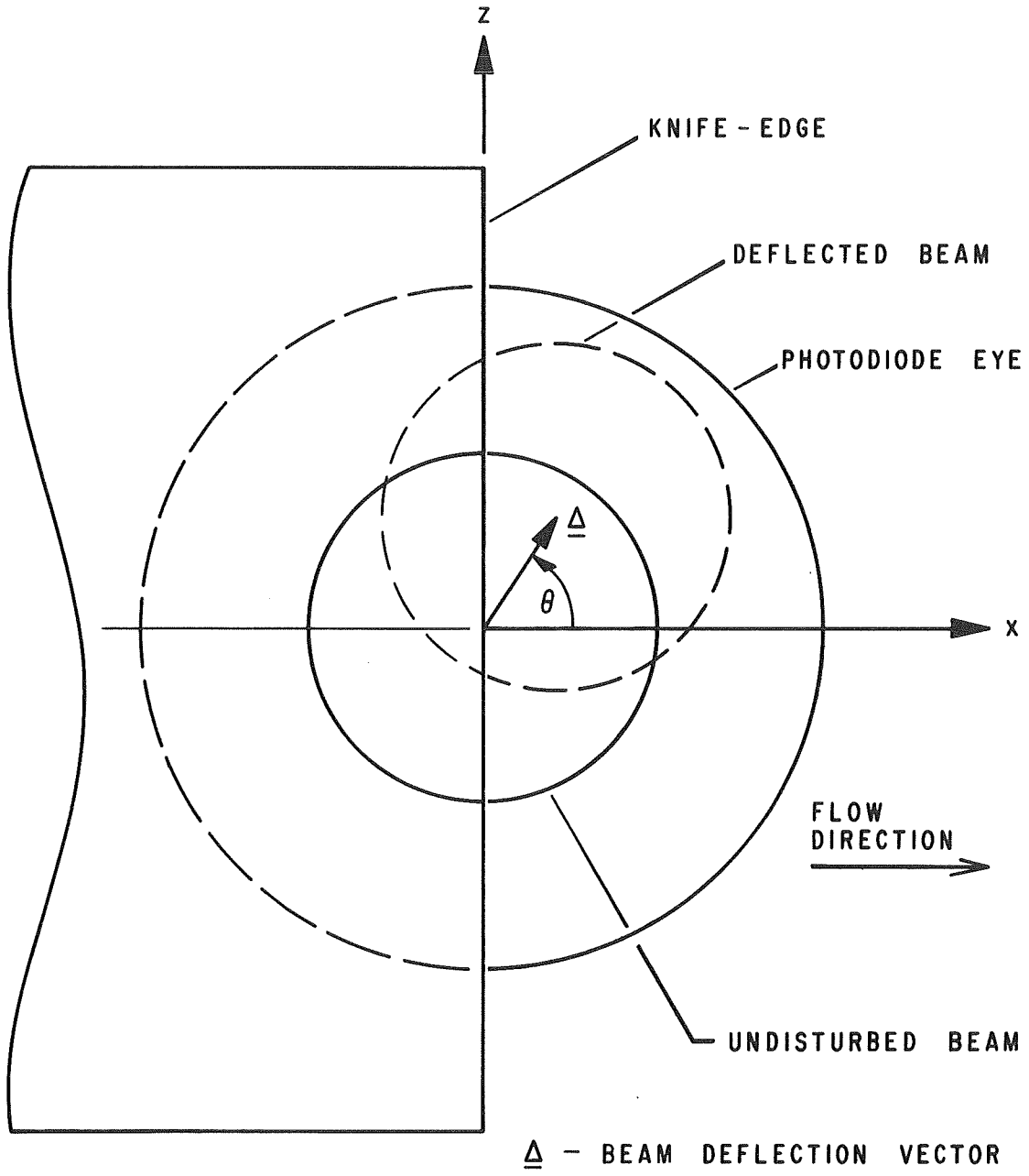

Figure 2. A Schematic of A Cross Section Taken Across One Beam of A Laser Schlieren System.

where the first group of terms in brackets on the right-hand side of equation (2) is the change in the output signal per unit change in Δ_x and is assumed to be a constant, C.

$$i(t) = C \cdot \Delta_x(t) \ . \tag{3}$$

For this case, the photodetector output is a linear function of the component of $\underline{\Delta}$ which is normal to the knife-edge. This result is not unrealistic and can be approximated very well in practice.

Since

$$\Delta_x(t) = \Delta(t) \cdot \cos \theta(t), \tag{4}$$

equation (3) can be expressed as

$$i(i) = C \cdot \Delta(t) \cdot \cos \theta(t). \tag{5}$$

Thus, we see from equation (5) that i(t) is a function of the direction as well as the magnitude of the beam deflection vector.

For the laser schlieren system shown in figure 1, the signals from the photodetectors monitoring the respective beams are

$$i_a(t) = C_a \cdot \Delta_a(t) \cdot \cos \theta_a(t) \tag{6}$$

and

$$i_b(t) = C_b \cdot \Delta_b(t) \cdot \cos \theta_b(t). \tag{7}$$

Let us assume that the turbulence is two-dimensional; i.e., the time-averaged statistical properties do not vary along the beams. Although this assumption will restrict the analysis, it provides a better model for the purpose of describing the fundamental concept, the prime purpose here. It will soon become evident that relaxing this assumption will not change the fundamental relationship between the shape of the correlograms and the angular velocity of the density gradient vector component which is normal to the respective beams.

The cross-correlation of the signals $i_a(t)$ with $i_b(t + \tau)$ is given by

$$R(\xi,\tau) = \lim_{T\to\infty} \frac{1}{T} \int_0^T i_a(t) \cdot i_b(t+\tau)\, dt. \tag{8}$$

Let us substitute equations (6) and (7) into (8) and assume that the integration time, T, is large enough so that

$$R(\xi,\tau) = \frac{C_a C_b}{T} \int_0^T \triangle_a(t) \cdot \triangle_b(t+\tau) \cdot \cos\theta_a(t) \cdot \cos\theta_b(t+\tau)\, dt. \tag{9}$$

Figure 3 shows the knife-edge orientation for the cross-correlation of equation (9). This figure also shows the beam deflection vector of beam A at time t when a particular disturbance is passing through the beam, and, the $\underline{\triangle}$ of beam B when the same disturbance is passing through beam B at a later time $t + \tau$. When this disturbance passes through beam A, the beam is deflected in a direction θ_a, and by a magnitude of $\triangle_a$. This magnitude of the deflection vector is determined by the magnitude of the density gradient component normal to the beam characterizing the disturbance. The direction of the deflection is due to the particular orientation of the same density gradient component. If we make the realistic assumption that the disturbance rotates as it travels downstream, its orientation will not necessarily be the same when it passes through beam B as it was when it passed through beam A. This is represented in figure 3 where the beam deflection vector caused by a particular disturbance has rotated during its transit from beam A to beam B. It follows that

$$\left| \underline{\triangle}_a(t) \times \underline{\triangle}_b(t+\tau) \right| = \triangle_a(t) \cdot \triangle_b(t+\tau) \cdot \sin\phi(t+\tau). \tag{10}$$

This equation defines the angle ϕ through which the disturbance rotated during transit from beam A to B. Thus,

$$\phi(t+\tau) = \theta_a(t) - \theta_b(t+\tau). \tag{11}$$

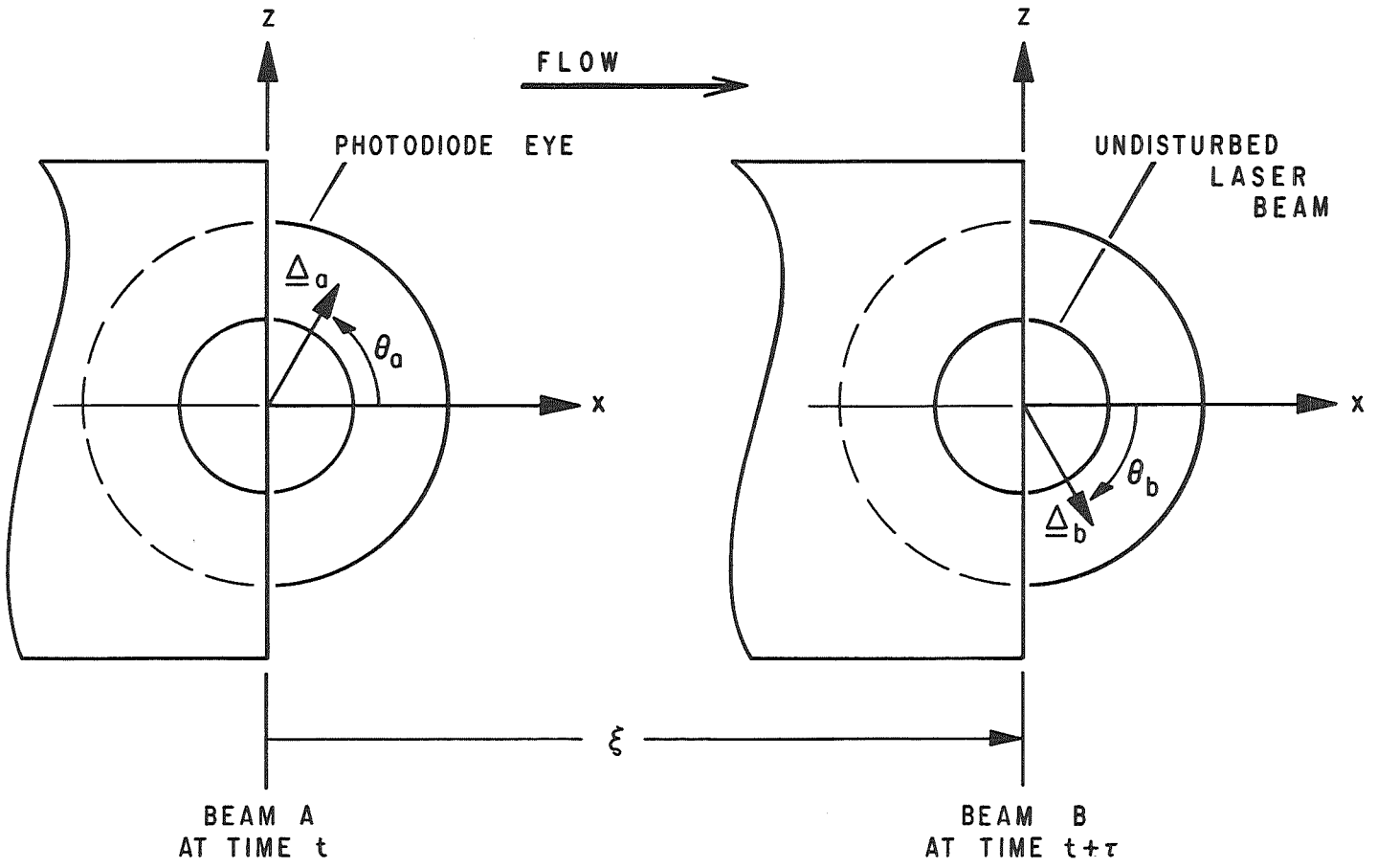

Figure 3. A Schematic of A View Taken Along Laser Beams of The Laser Schlieren System Shown in Figure 1.

Solving equation (11) for $\theta_b(t+\tau)$ and substituting into equation (9) gives

$$R(\xi,\tau) = \frac{C_a C_b}{T} \int_o^T \triangle_a(t) \cdot \triangle_b(t+\tau) \cdot \cos\,\theta_a(t) \cdot \cos[\theta_a(t) - \phi(t+\tau)]dt. \tag{12}$$

To examine the effect which this angular rotation has upon the cross-correlation function $R(\xi,\tau)$, let us consider a simplified two-dimensional flow model where it is assumed that the disturbances are random and produce statistically stationary signals. The cross-correlation function (equation (12)) will be studied for two cases: (a) where the disturbances do not rotate and (b) where each disturbance rotates through the same angle, ϕ, during transit from beam A to beam B. Case (a) will be discussed first.

Figure 4 shows four knife-edge arrangements where the view is taken along the laser beams similar to that of figure 3. The differences between these four figures is the orientation of the downstream knife-edge. If we assume that the disturbances do not rotate, then

$$\phi(t+\tau) = 0, \tag{13}$$

and from equation (11), we see that

$$\theta_b(t+\tau) = \theta_a(t). \tag{14}$$

The signal from beam A will be

$$i_a(t) = C_a \cdot \triangle_a(t) \cdot \cos\,\theta_a(t) \tag{15}$$

and is the same for all four knife-edge arrangements.

The signal from beam B, for figures 4a,b,c, and d are

$$i_{b1}(t+\tau) = C_b \cdot \triangle_b(t+\tau) \cdot \cos\,\theta_b(t+\tau) \tag{16}$$

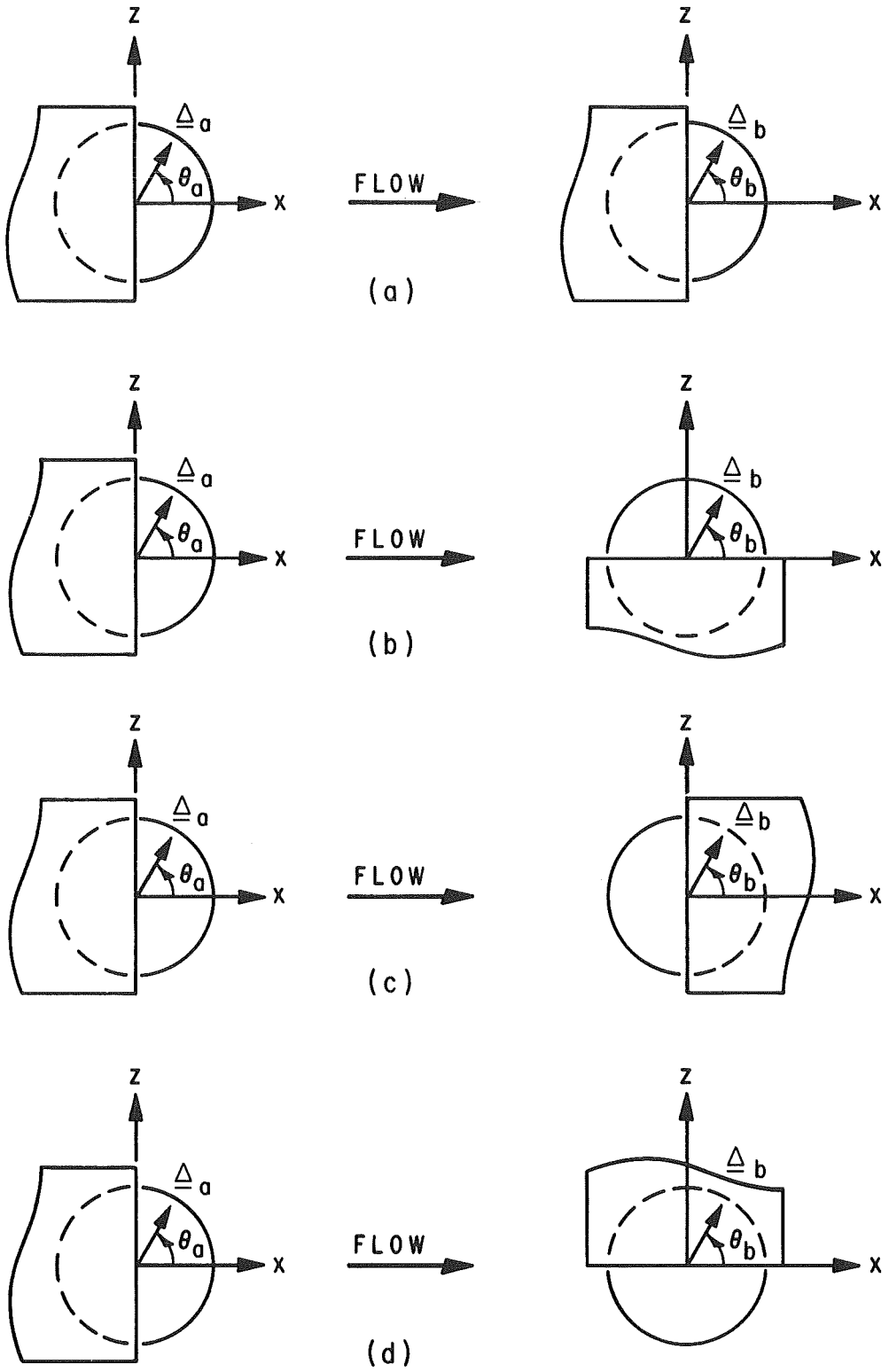

Figure 4. A Schematic of Four Knife-Edge Arrangements of The Laser Schlieren System Shown in Figure 1.

$$i_{b2}(t+\tau) = C_b \cdot \Delta_b(t+\tau) \cdot \sin \theta_b(t+\tau) \tag{17}$$

$$i_{b3}(t+\tau) = -C_b \cdot \Delta_b(t+\tau) \cdot \cos \theta_b(t+\tau) \tag{18}$$

$$i_{b4}(t+\tau) = -C_b \cdot \Delta_b(t+\tau) \cdot \sin \theta_b(t+\tau), \tag{19}$$

respectively.

When we substitute equation (14) into equation (16), (17), (18) and (19), the cross-correlation functions for the respective knife-edge arrangements become

$$R_1(\xi,\tau) = \left[\frac{C_a C_b}{T}\right] \int_0^T \Delta_a(t) \cdot \Delta_b(t+\tau) \cdot \cos \theta_a(t) \cdot \cos \theta_a(t)\, dt \tag{20}$$

$$R_2(\xi,\tau) = \left[\frac{C_a C_b}{T}\right] \int_0^T \Delta_a(t) \cdot \Delta_b(t+\tau) \cdot \cos \theta_a(t) \cdot \sin \theta_a(t)\, dt \tag{21}$$

$$R_3(\xi,\tau) = -\left[\frac{C_a C_b}{T}\right] \int_0^T \Delta_a(t) \cdot \Delta_b(t+\tau) \cdot \cos \theta_a(t) \cdot \cos \theta_a(t)\, dt \tag{22}$$

$$R_4(\xi,\tau) = -\left[\frac{C_a C_b}{T}\right] \int_0^T \Delta_a(t) \cdot \Delta_b(t+\tau) \cos \theta_a(t) \cdot \sin \theta_a(t)\, dt. \tag{23}$$

The cross-correlograms for these arrangements are shown in figures 5a, 5b, 5c, and 5d, respectively. An example of a cross-correlogram, represented by equation (20), would be similar to that shown in figure 6a. A cross-correlogram similar to that represented by equation (22) is shown in figure 6b.

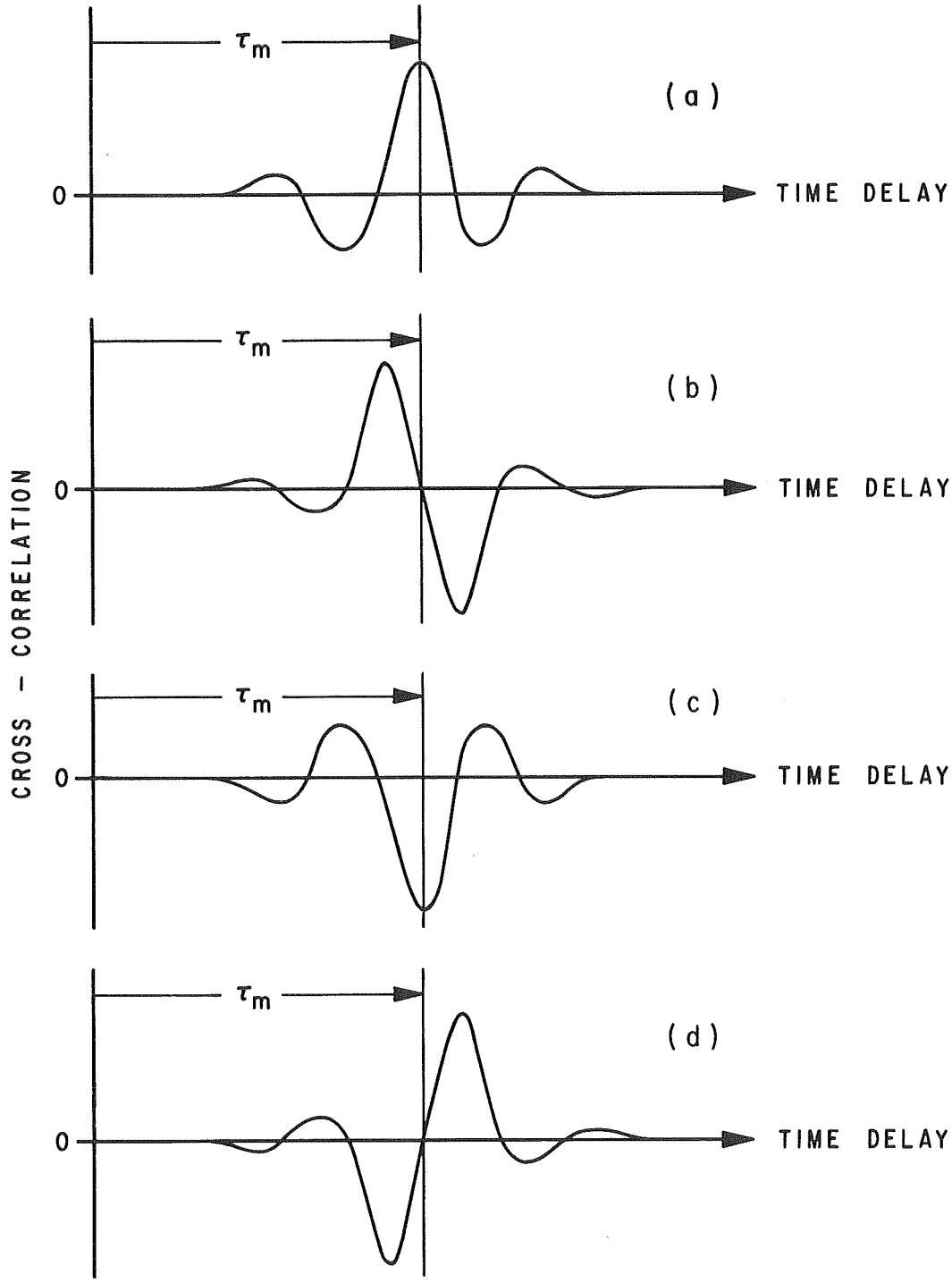

Figure 5. Schematic of Cross-Correlograms Corresponding to the Knife-Edge Arrangements in Figure 4, Respectively.

(a)

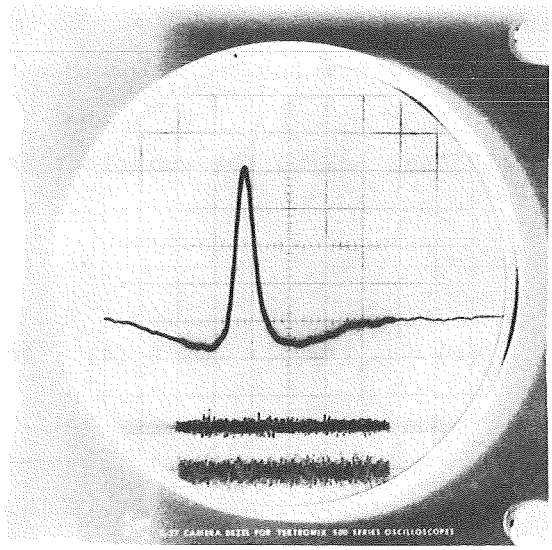

CROSS-CORRELATION

TIME DELAY

(b)

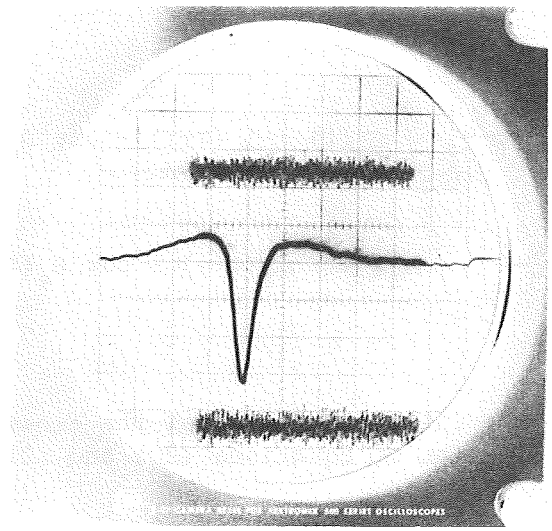

CROSS-CORRELATION

TIME DELAY

Figure 6(a). Typical Cross-Correlogram for Knife-Edge Arrangement of Figure 4(a) (Equation 20).
(b). Typical Cross-Correlogram for Knife-Edge Arrangement of Figure 4(c) (Equation 22).

For case B, it is assumed that each disturbance rotates through the same angle ϕ during transit from beam A to B; then,

$$\phi(t+\tau) = \phi. \tag{24}$$

Expanding equation (12) and making the substitution from equation (24), we get

$$R(\xi,\tau) = \left[\frac{C_a C_b}{T}\right] \int_o^T \Delta_a(t) \cdot \Delta_b(t+\tau) \cdot \cos^2\theta_a(t) \cdot \cos\phi \, dt$$

$$+ \left[\frac{C_a C_b}{T}\right] \int_o^T \Delta_a(t) \cdot \Delta_b(t+\tau) \cdot \cos\theta_a(t) \cdot \sin\theta_a(t) \cdot \sin\phi \, dt. \tag{25}$$

Since ϕ is not a function of time, cos ϕ and sin ϕ can be taken outside of the integrals on the right-hand side of equation (25), respectively.

$$R(\xi,\tau) = [\cos\phi]\left[\frac{C_a C_b}{T}\right] \int_o^T \Delta_a(t) \cdot \Delta_b(t+\tau) \cdot \cos^2\theta_a(t) \, dt$$

$$+ [\sin\phi]\left[\frac{C_a C_b}{T}\right] \int_o^T \Delta_a(t) \cdot \Delta_b(t+\tau) \cdot \cos\theta_a(t) \cdot \sin\theta_a(t) \, dt. \tag{26}$$

In equation (26), the integrals represent the cross-correlations derived for case A. Substitution of equations (20) and (21) into (26) yields

$$R(\xi,\tau) = [\cos\phi] \, R_1(\xi,\tau) + [\sin\phi] \, R_2(\xi,\tau). \tag{27}$$

Equation (27) relates the cross-correlogram of case B to those of case A. We see from equation (27) that

$$R(\xi,\tau) = R_1(\xi,\tau), \qquad \text{for } \phi = 0 \tag{28}$$

$$R(\xi,\tau) = R_2(\xi,\tau), \qquad \text{for } \phi = \pi/2 \tag{29}$$

$$R(\xi,\tau) = -R_1(\xi,\tau), \qquad \text{for } \phi = \pi \tag{30}$$

$$R(\xi,\tau) = -R_2(\xi,\tau), \qquad \text{for } \phi(3/2)\ \pi \tag{31}$$

as should be expected.

In equation (27) the unknown quantity is the angle ϕ. A direct measurement of ϕ for the idealized model in case B can be made by combining case A with case B. This procedure is referred to here as the method of "forced similarity" and is as follows:

(1) Compute the cross-correlogram $R(\xi,\tau)$ for zero beam separation with the knife-edges as shown in figure 2 ($\xi = 0$). Since $\phi = 0$ for $\xi = 0$,

$$R(0,\tau) = R_1(0,\tau). \tag{32}$$

(2) Separate the two beams by moving beam B downstream a known distance ξ from beam A. The position and knife-edge angle, ψ_a, of beam A are not changed ($\psi_a = 0$).

(3) Rotate the downstream knife-edge, B, to the angle ψ_{bm} which produces the same "shape" of the cross-correlogram as was computed for zero beam separation. For this simplified flow model, the angle ψ_{bm} corresponding to the maximum "degree of similarity" between the cross-correlograms is equal to the angle ϕ through which the disturbances rotate during transit from beam A to beam B. The "forced similarity" condition is

$$R(\xi,\tau - \tau_m,\psi_b) = K(\xi,\tau,\psi_b) \cdot R(0,\tau) \tag{33}$$

where $K(\xi,\tau,\psi_b)$ is "optimum" when $\psi_b = \psi_{bm}$ for a particular ξ.

(4) The most probable transit time τ_m of the disturbances is determined by the time delay on the cross-correlogram for separated

beams corresponding to the similar position at zero time delay on the cross-correlogram for zero beam separation.

(5) The most probable speed of the disturbances is

$$<U> \doteq \xi \ \tau_m. \tag{34}$$

(6) The most probable angular velocity is

$$<\underline{\omega}_p> \doteq \emptyset\tau_m = \psi_{bm}\tau_m. \tag{35}$$

These models have been used to relate the experimentally observed skewness of cross-correlograms, computed from laser schlieren signals, to the rotation of the turbulent structures.

III. PRACTICAL APPLICATION OF THE METHOD OF FORCED SIMILARITY

In the previous section a method of "forced similarity" was introduced which provides the means for measuring the most probable preferred angular velocity of the simplified two-dimensional disturbances. As a consequence of the proposed relation between the skewness of the cross-correlogram and the rotational motion of the disturbances, the "forced similarity" condition, equation (33), must be imposed in order to determine the most probable transit time, τ_m, as well as all other statistical properties which are computed from the shape of the cross-correlogram in the neighborhood of τ_m. Imposing this condition analytically involves normalization of the cross-correlogram and optimization of the similarity function, $K(\xi,\tau,\psi_b)$. These details will not be discussed here. Rather, we will proceed to the practical application.

Figure 7 shows a schematic of the free jet shear layer of a supersonic axisymmetric air jet. Two laser beams are directed through the flow perpendicular to one another and in such a manner that the plane formed by the beams is perpendicular to the centerline of the jet. The horizontal beam (beam A) passes through the center of the jet. The vertical beam (beam B) passes through the shear layer and intersects the horizontal beam as shown in figure 7.

In reference 4 it is theoretically shown that the statistical cross-correlation of the signals from two such beams should result in a cross-correlogram representative of the components of the signals which are

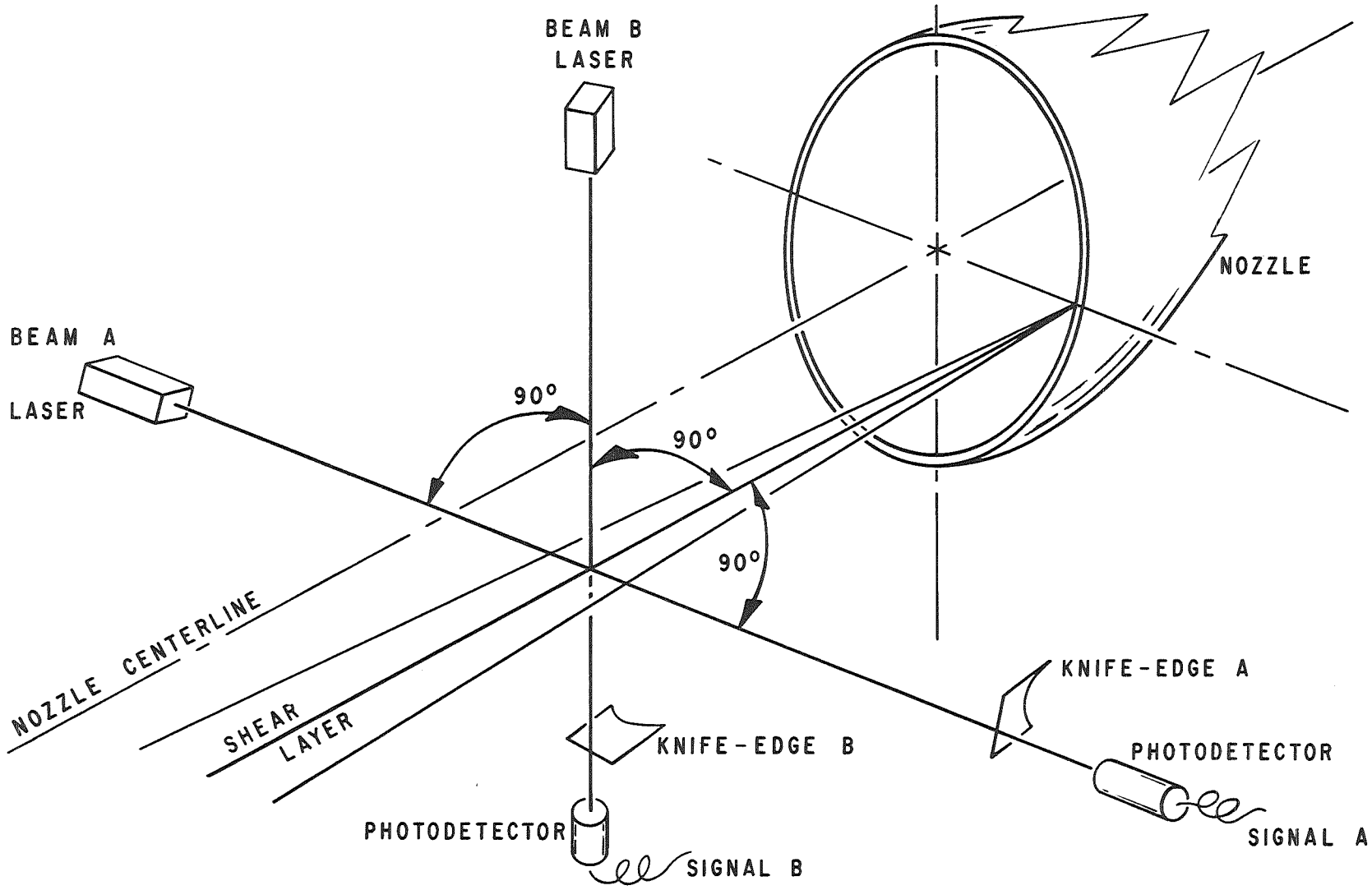

Figure 7. Cross-Beam Arrangement for Axisymmetric Jet

caused by disturbances passing through the localized region about the beam intersection. That is, flow disturbances passing through the beams that are not common to both beams do not contribute significantly to the cross-correlogram (the integration time being sufficiently long). In reference 2 the experimental verification of this "cross-beam" concept was successfully achieved in a supersonic (M = 2.0) turbulent wake of a thin flat plate.

Referring again to the axisymmetric jet, the "forced similarity" condition may be satisfied for retrieving all three components of the most probable preferred angular velocity $\langle \underline{\omega}_p \rangle$, of the disturbances passing through a localized region of the shear layer. We may assume that the mean statistical properties of the turbulence are also axisymmetric, and thereby eliminate one component of $\langle \underline{\omega}_p \rangle$. However, this is not necessary and will not be done.

The experimental procedure is as follows:

(1) The beams are directed through the turbulence as shown in figure 7 with zero beam intersection ($\xi = 0$). The knife-edges are positioned as shown ($\psi_a = 0$ and $\psi_b = 0$).

(2) The cross-correlogram $R(0,\tau)$ is computed.

(3) The vertical beam (beam B) is moved downstream a distance ξ as shown in figure 8, and the cross-correlogram $R(\xi,\tau)$ is computed which satisfies the "forced similarity" condition

$$R(\xi,\tau - \tau_m,\psi_{am},\psi_{bm}) = K(\xi,\tau,\psi_{am},\psi_{bm}) \cdot R(0,\tau) \tag{36}$$

for axisymmetric flows. $K(\xi,\tau,\psi_{am},\psi_{bm})$ is determined to be the "weakness" function necessary to satisfy equation (36) in the neighborhood of τ_m. Experimentally, this involves rotation of both of the knife-edges. When this step is completed the condition should be satisfied for this particular flow.

(4) If necessary, the next step would be to rotate the downstream beam in the plane perpendicular to the centerline of the jet. This is done in increments and step (3) is repeated for each increment until all three angles ψ_a, ψ_b, and ψ_c have been determined which satisfy the three-dimensional similarity condition

$$R(\xi,\tau - \tau_m,\psi_{am},\psi_{bm},\psi_{cm}) = K(\xi,\tau,\psi_{am},\psi_{bm},\psi_{cm}) \cdot R(0,\tau) \tag{37}$$

where ψ_c is the angle of rotation of the vertical beam.

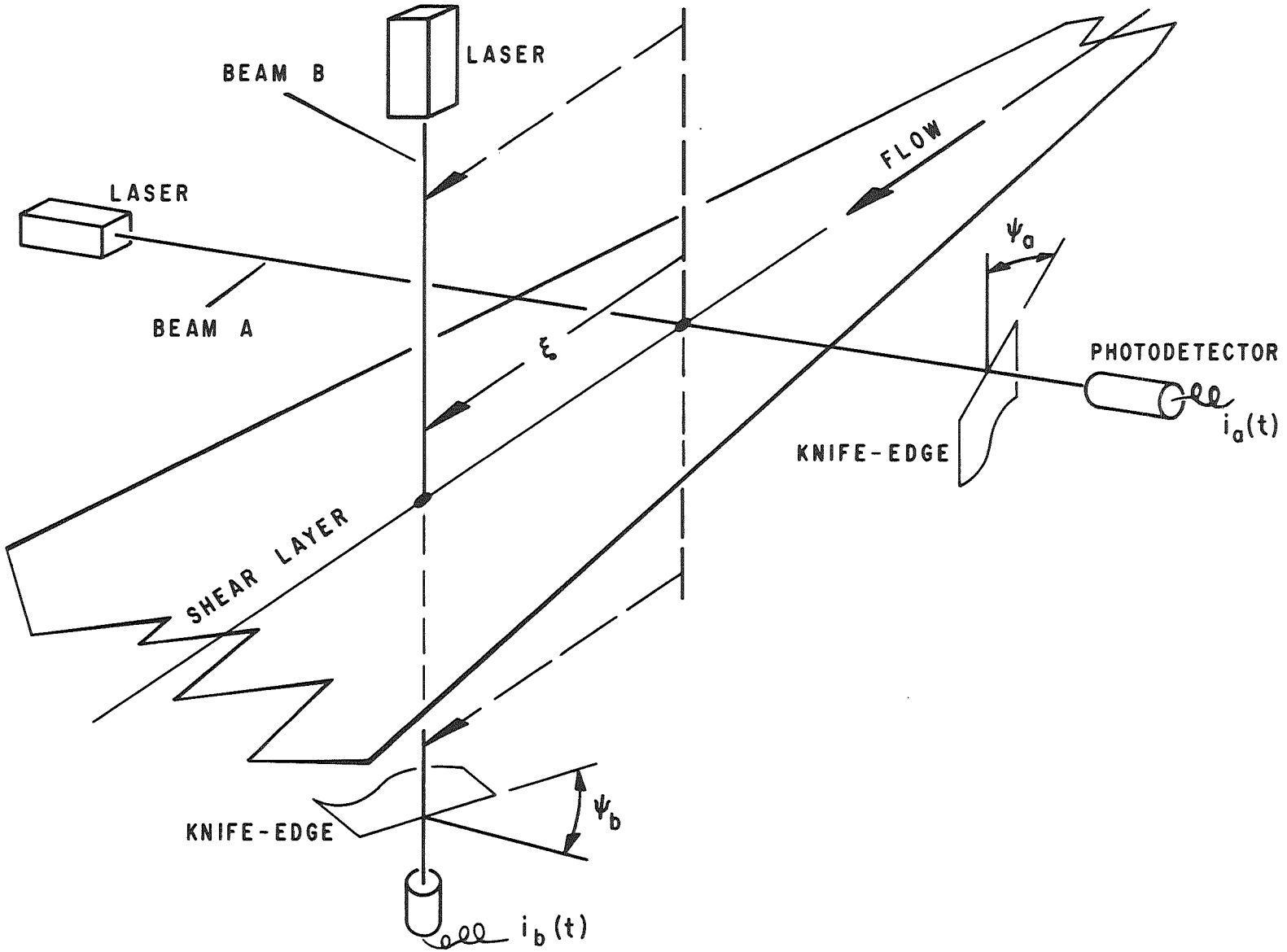

Figure 8. Schematic of Space-Time Correlation Satisfying the "Forced Similarity" Condition.

(5) The most probable transit time of the disturbances is determined by evaluating the similarity condition (37) for $\tau = 0$:

$$R(\xi, 0 - \tau_m, \psi_{am}, \psi_{bm}, \psi_{cm}) = \frac{R(0,0)}{K(\xi, 0, \psi_{am}, \psi_{bm}, \psi_{cm})} . \tag{38}$$

Thus, τ_m is equal to the time delay on the cross-correlogram $R(\xi, \tau, \psi_{am}, \psi_{bm}, \psi_{cm})$ corresponding to the similar position at zero time delay on the cross-correlogram for zero beam separation.

(6) The components of the most probable preferred angular velocity are

$$\langle \omega_x \rangle \doteq \frac{\psi_{cm}}{\tau_m} \tag{39}$$

$$\langle \omega_y \rangle = \frac{-\psi_{am}}{\tau_m} \tag{40}$$

$$\langle \omega_z \rangle = \frac{\psi_{bm}}{\tau_m} \tag{41}$$

and the most probable vector is

$$\langle \underline{\omega}_p \rangle = \hat{i} \langle \omega_x \rangle + \hat{j} \langle \omega_y \rangle + \hat{k} \langle \omega_z \rangle. \tag{42}$$

(7) The most probable speed of transit is

$$\langle U \rangle = \frac{\xi}{\tau_m} . \tag{43}$$

Figures 9 and 10 show the first successful cross-beam measurements made in the supersonic free shear layer of an axisymmetric jet. The exit Mach number of the nozzle was 2.5, and the expansion was optimum.

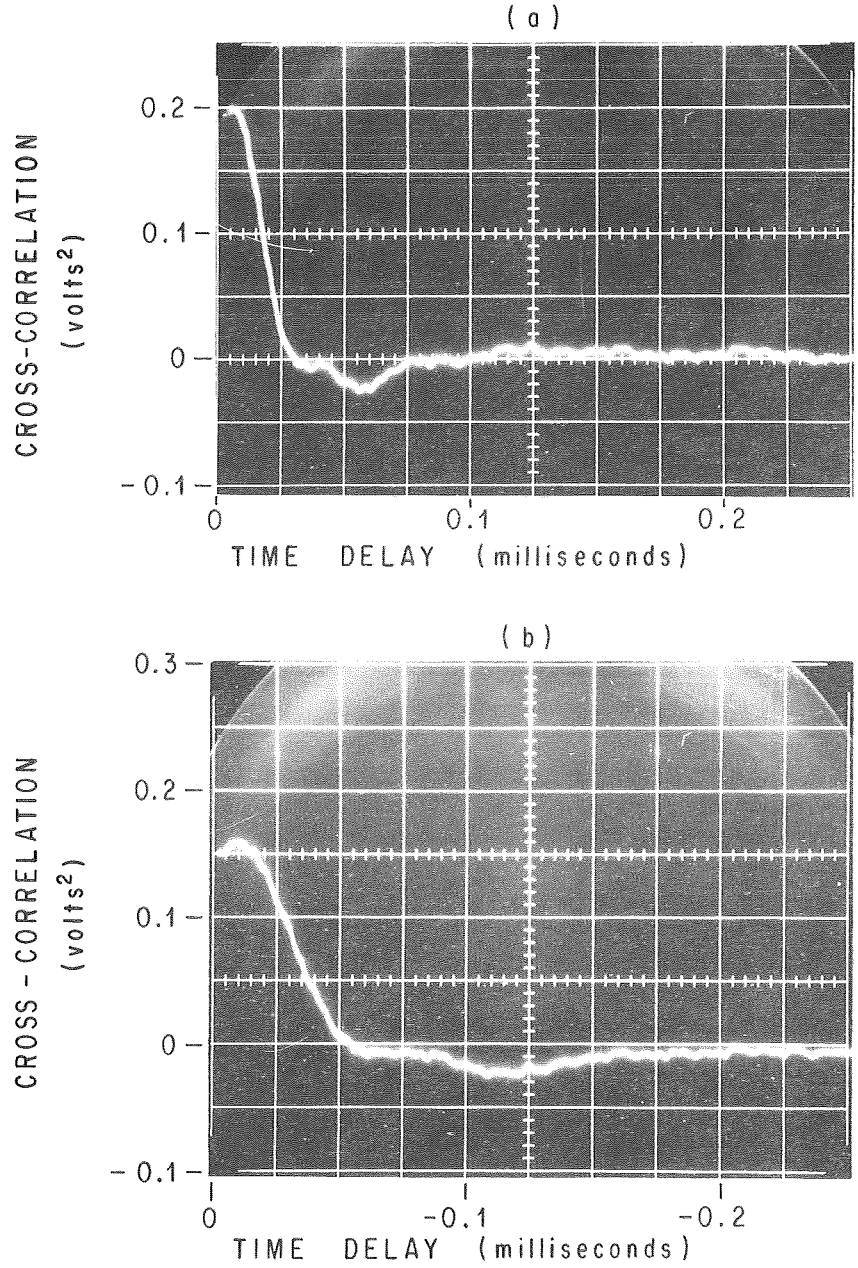

Figure 9. Cross-Correlogram Computed from Laser Schlieren Signals Retrieved from Free Shear Layer of Axisymmetric Jet (M_e = 2.5).
(a) Positive Time Delay Range
(b) Negative Time Delay Range

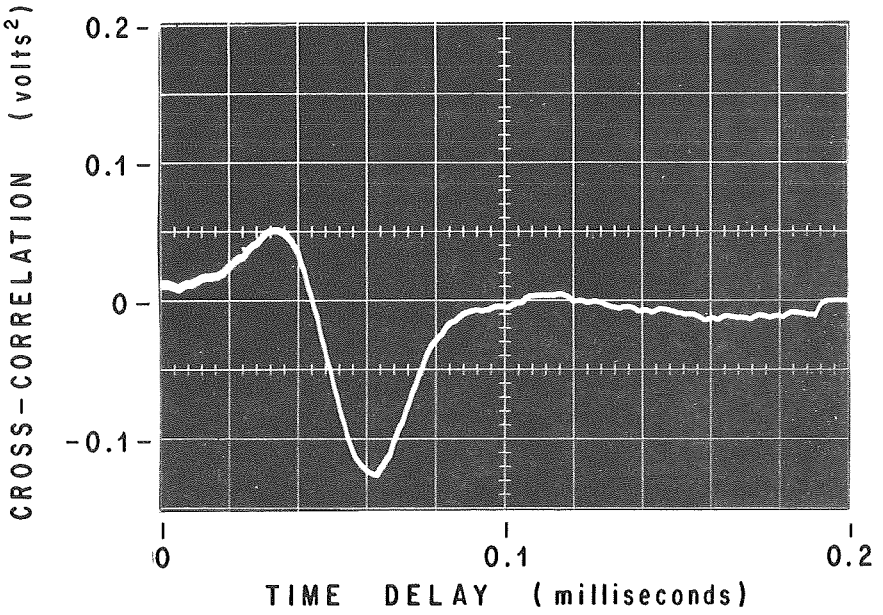

Figure 10. Cross-Correlogram Computed for Same Case as That of Figure 9 Except Beams are Separated by 1.0 Inch as Shown in Figure 8 ($\psi_a = 0$, $\psi_b = 0$).

In figures 9a and 9b, the positive and negative time delay ranges of the cross-correlogram are shown. The beam geometry is shown in figure 7 ($\xi = 0$). It can be seen that the correlogram is not symmetric about the origin ($\tau = 0$), but that there is a dominant peak at ($\tau = 0$). This cross-correlogram corresponds to $R(0,\tau)$ in equation (36).

Figure 10 shows the cross-correlogram for a beam separation of one inch ($\xi = 1"$) with the knife-edges in the same positions as in figure 9 ($\psi_a = 0$, $\psi_b = 0$). The fact that there is a considerable difference in the shapes of these correlograms satisfies one necessary condition required by the theory of "forced similarity."

Figure 11 shows four cross-correlations computed from signals retrieved with a laser schlieren system using parallel beams as previously described. The data* were retrieved from the supersonic ($M = 2.0$) turbulent boundary layer on the thin plate shown in figure 12. The beams were separated by approximately 1.5 inches in the direction of flow and were approximately 1/8 inch above the surface of the plate. These cross-correlograms were computed with the downstream knife-edge orientations shown and were the first experimental attempt to relate the shape of the correlogram, in the neighborhood of the most probable transit time, τ_m, to the orientation of the knife-edges relative to the flow and to each other.

These data show that the relative orientation of the knife-edges to each other does indeed influence the shape of the cross-correlogram. Therefore, it is reasonable to consider that the cross-correlogram is influenced by a change in the relative orientation of the disturbances to the knife-edges as they translate from one to the other.

IV. CONCLUSIONS

Based upon the theoretical and experimental results which have been presented, the following conclusions are:

(1) The relative orientation of the knife-edges to each other controls the shape of the cross-correlogram in the neighborhood of the time delay, τ_m, corresponding to the most probable transit time of disturbances between the laser beams.

---

*These measurements were made in MSFC's Bisonic Wind Tunnel on June 3, 1969 [2].

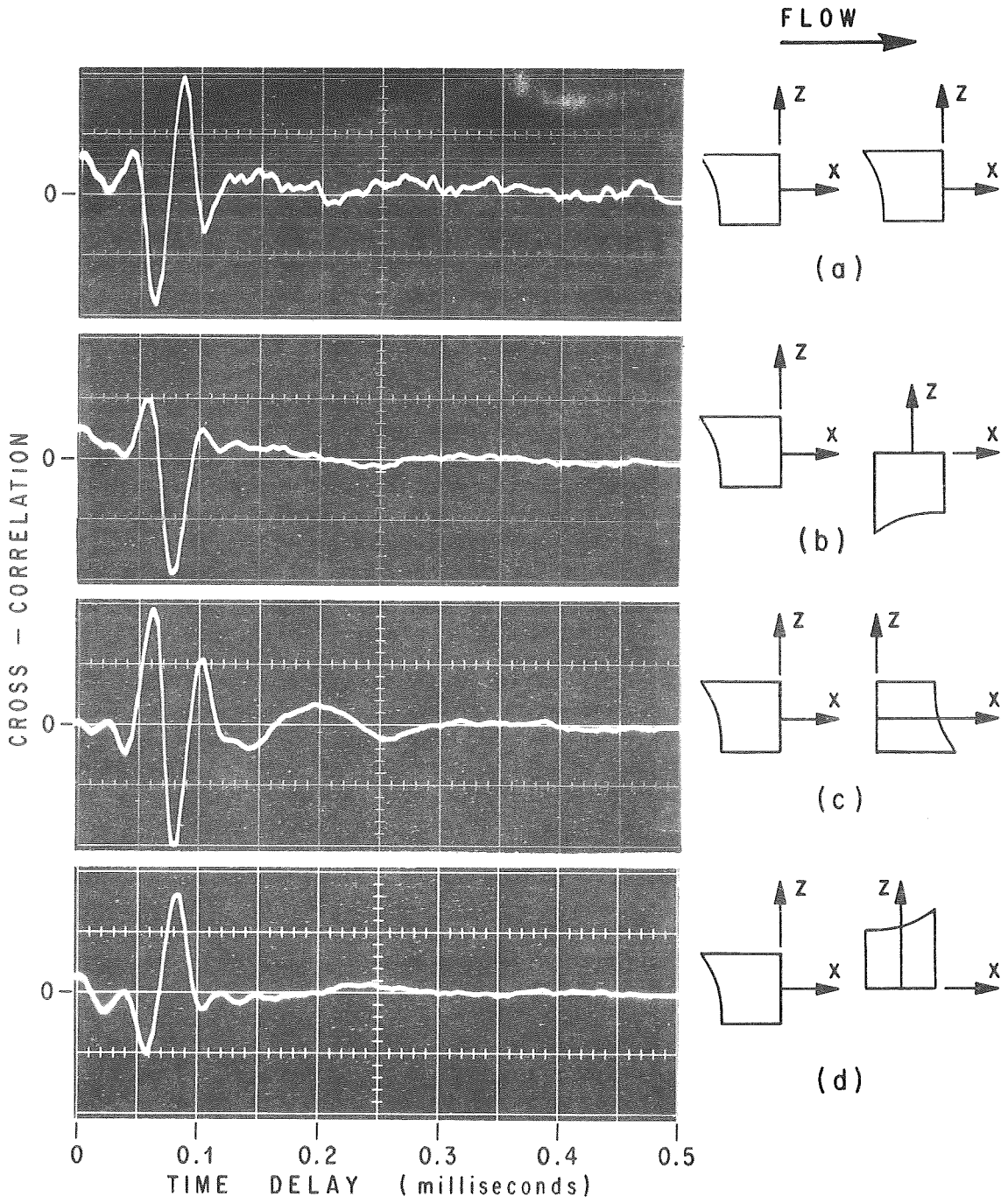

Figure 11. Cross-Correlograms Computed for Four Knife-Edge Arrangements as Shown.

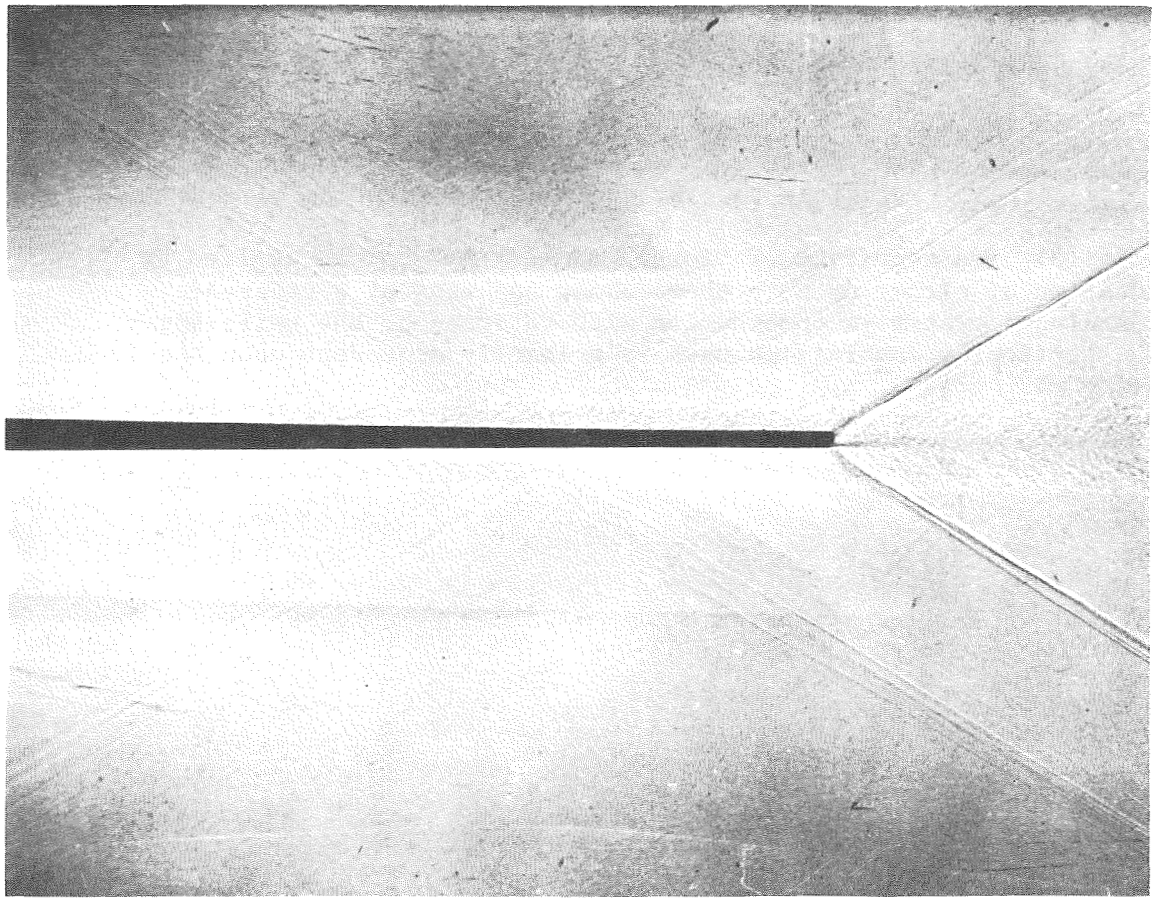

Figure 12. Shadowgraph of Flow Field Generated by the Thin Plate Model

(2) The method of "forced similarity" introduced here provides the means for separating the translational and rotational contributions to the shape of the cross-correlogram. However, more experimental results are needed for verification.

(3) The "forced similarity" condition is based upon the assumption that the shape of the cross-correlogram computed with beams separated is "similar" to that computed with zero beam separation when the contribution due to rotation has been eliminated (the effect of decay accepted).

(4) Because of the rotational influences, significant error can result in the flow properties which are computed from the shape of the cross-correlogram unless the influence due to rotation is considered.

(5) The condition of "forced similarity" may be applied by rotation of either or both beams about the axes of a reference coordinate system in combination with rotation of the knife-edges. The particular combination used is primarily dependent upon the flow.

REFERENCES

1. Bendat, J. S. and A. G. Pierson, Measurement and Analysis of Random Data, John Wiley, New York, 1966.

2. Funk, B. H. and H. A. Cikanek, Jr., "Optical Probing of Supersonic Aerodynamic Turbulence with Statistical Correlation. Phase I: Feasibility," NASA TM X-53850, June 9, 1969.

3. Cambel, A. B. and B. H. Jennings, Gas Dynamics, McGraw-Hill Book Co., Inc., New York, 1958.

4. Fisher, M. J. and F. R. Krause, "The Cross Beam Correlation Technique," J. Fluid Mech. (1967), Vol. 28, part 4, pp. 705-717.

A DIRECT MEASUREMENT OF THE MOST PROBABLE PREFERRED ANGULAR VELOCITY OF TURBULENT STRUCTURES BY OPTICAL CORRELATION OF LASER SCHLIEREN SIGNALS

by B. H. Funk

The information in this report has been reviewed for security classification. Review of any information concerning Department of Defense or Atomic Energy Commission programs has been made by the MSFC Security Classification Officer. This report, in its entirety, has been determined to be unclassified.

This document has also been reviewed and approved for technical accuracy.

W. K. Dahm
Chief, Aerophysics Division

E. D. Geissler
Director, Aero-Astrodynamics Laboratory

MSFC—RSA, Ala

DISTRIBUTION

DIR
Dr. von Braun
Mr. Shepherd

S&E-ASTR
Mr. Hoberg
Dr. Decher
Dr. Randall

S&E-COMP
Mr. E. Hopper
Mr. J. Jones

S&E-SSL
Mr. Heller
Mr. Snoddy
Mr. Shelton

S&E-AS
Mr. Williams
Mr. Thomae
Mr. Scott

S&E-R
Dr. W. Johnson
Mr. Miles
Mr. Attaya
Mr. Hopper
Mr. Adams

S&E-ASTN-PTD
Mr. Hopson

PM-DIR

PM-AA
Mr. Belew

MS-IP
MS-IL (8)
A&TS-MS-D, Mr. Goldston
MS-H
DEP-T
CC
A&TS-TU (6)
PM-PR-M

A&TS-PAT
Mr. L. Wofford, Jr.

AD-S

PM-CO-CH
Col. Hirsch

S&E-AERO
Dr. Geissler
Mr. Horn
Mr. Bean
Mr. Murphree
Mr. Butler
Mr. von Puttkamer
Dr. Heybey
Mr. Cummings
Dr. DeVries
Mr. Lovingood
Mr. Rheinfurth
Mr. Jandebeur
Mr. Dahm
Mr. Holderer
Mr. Wilson
Mr. Linsely
Mr. Felix
Mr. Reed
Mr. Lindberg
Mr. W. Vaughan
Mr. Turner
Mr. Kaufman
Mr. Huffaker
Mr. Schutzenhofer
Mr. Forney
Mr. Burkett
Mr. Few
Mr. Johnston
Mr. Wilhold
Mr. J. Jones
Mr. Struck
Mr. Sims
Mr. Greenwood
Mr. Brewer
Mr. I. Jones
Mr. Ellner
Mr. Heaman
Mrs. Hightower

DISTRIBUTION (Continued)

S&E-AERO (cont'd)
Mr. W. Davis
Mr. Carter
Mr. Simon
Mr. Neighbors
Mr. Bush
Mr. Belew
Mr. Ballance
Mr. Cliff
Dr. F. Krause (25)
Mr. Pickelner
Mr. Funk (50)

EXTERNAL

Tech. & Sci. Info. Facility (25)
Box 33
College Park, Md.
Attn: NASA Rep. (S-AK/RKT)

NASA Headquarters (2)
Washington, D. C. 20546
Attn: Director of OART
RAO, Mr. McGowan
RV-I, Mr. Cerreta
SAB, Mr. George
REI, Dr. Menzel
RV-2, Mr. Michel
RAA, Mr. Parkinson
RAP, Mr. Rekos
RRF, Mr. Schwartz
SM, Mr. Badgley
RF, Mr. Ginter
SAR, Dr. Summers
RD-A, Mr. Harper
SM, Mr. Brockman
SV, Mr. Salmanson
SFM, Mr. Spreen
SF, Mr. Tepper
RVI, Mr. DeMeritt
RVI, Mr. Green
MA, Mr. Reiffel
RV-2, Mr. Rosche
RR, Dr. Kurzweg
RRP, Mr. Danberg
MTP, Mr. Peil
RVA, Mr. Underwood
REI, Mr. Vacca

NASA - Langley Res. Center (2)
Langley Field
Hampton, Va. 23365

NASA - Goddard Space Flt. Center (2)
Greenbelt, Md. 20771

NASA - Flt. Res. Center (2)
Edwards, Calif. 93523

NASA - Ames Res. Center (2)
Moffett Field
Mountain View, Calif. 94035

NASA - Lewis Res. Center (2)
21000 Brookpark Rd.
Cleveland, Ohio 44135

NASA - JFK Space Center (2)
Kennedy Space Center, Fla. 32899

Jet Propulsion Lab. (2)
Calif. Inst. of Tech.
4800 Oak Grove Dr.
Pasadena, Calif. 91103

Rocketdyne
6630 Canoga Ave.
Canoga Park, Calif. 91304
Attn: R. L. Proffit
G. L. Cline

ESSA
National Bureau of Standards Bldg.
Boulder, Colorado 80302
Attn: Dr. B. Bean
Mr. McGavin
Dr. G. Little
Mr. Abshire
Mr. Sweezy
Dr. Derr

FAA - NO-10
800 Independence Ave. SW
Washington, D. C. 20590
Attn: Dr. K. Power
Dr. J. Powers

A&M College
Normal, Ala. 35762
Atn: Prof. H. Foster
Mr. J. Shipman
Mr. C. Foster

University of Oklahoma
College of Engr.
Norman, Okla. 73069
Attn: Dean F. Block
Dr. Canfield
Dr. Fowler
Dr. Day
Mr. Lisobey

Dr. Lin
University of Wisconsin
Madison, Wisconsin

Mr. Ajit Kumar Ray
Univ. of Ottawa
Dept. of Math.
Ottawa 2, Canada

Mr. A. S. Mujumdar
Pulp & Paper Res. Inst. of Canada
570 St. John's Rd.
Pointe-Claire, P. Q.
Canada

Mr. T. W. Kao
Dept. of Space Sci. & Appl. Phys.
The Catholic Univ. of America
Washington, D. C. 20017

Dr. J. E. Mitchell
Esso Res. & Eng. Co.
P. O. Box 45
Linden, N. J. 07036

Mr. Philemon Baw
Bureau of Engr. Res.
Rutgers - The State Univ.
College of Engr.
New Brunswick, N. J. 08903

Mr. Robert Torrest
Chem. Engr. Dept.
Univ. of Minnesota
Minneapolis, Minnesota 55455

Dr. M. A. Badri
Dept. of Aeronautical Engr.
Indian Inst. of Science
Bangalore-12, India

Mr. R. Antonia
The Univ. of Sydney
Dept. of Mech. Engr.
Sydney, N.S.W.
Australia

EXTERNAL DISTRIBUTION (Continued)

Dr. H. P. Pao
Dept. of Space Sci. & Appl. Phys.
The Catholic Univ. of America
Washington, D. C. 20017

Director
Cornell Aeronautical Lab., Inc.
P. O. Box 235
Buffalo, N. Y. 14221

Mr. Ta-jin Kuo
The Pa. State Univ.
Dept. of Aeronautical Engr.
233 Hammond Bldg.
Univ. Park, Pa.

Mr. Fritz Bien
Univ. of Calif. San Diego
Dept. of Aerospace & Mech. Engr. Sci.
P. O. Box 109
La Jolla, Calif. 92038

Lt. T. M. Weeks, FDME
Wright-Patterson AFB, Ohio 45433

Mr. Earl Logan, Jr.
Assoc. Prof. of Engr.
Arizona State Univ.
Tempe, Arizona

Prof. Geo. F. Carrier
Div. of Engr. & Appl. Phys.
Harvard Univ., Pierce Hall
Cambridge, Mass. 02138

Dr. Cohen
United Aircraft Res. Lab.
Silverlane East
Hartford, Conn.

Mr. D. Heckman
CARDE
P. O. 1427
Quebec, Canada

Mr. D. Ellington
CARDE
P. O. 1427
Quebec, Canada

U. S. Dept. of Interior
Bureau of Mines
Dr. Joseph M. Singer
Explosives Res. Center
4800 Forbes Ave.
Pittsburgh, Pa. 15213

Mr. J. L. Richardson
Mgr., Appl. Chem.
Aeroneutronic Div.
Philco Corp.
Ford Rd.
Newport Beach, Calif.

Dr. Srbislav Zivanovi
Senior Res. Engr.
Aerospace Operator
Defense Systems Div.
General Motors Corp.
6767 Hollister Ave.
Goleta, Calif.

Mr. S. Molder
McGill Univ.
805 Sherbrooke West
Montreal 2, Canada

Madame G. Comte-Bellot
Laboratories de Mecanique
des Fluides
Universite de Grenoble
44-46 Ave. Felix-Viallet
Grenoble, France

Mr. Roland E. Lee
Aerophysics Div.
U. S. Naval Ordnance Lab.
White Oak
Silver Spring, Md.

EXTERNAL DISTRIBUTION (Continued)

Mr. W. G. Tiederman
Shell Developments
Emeryville, Calif.

Director
Polytechnic Inst. of Brooklyn
Aerospace Engr.
527 Atlantic Ave.
Freeport, N. Y.

Dr. I. T. Osgerby
Hypervelocity Br.
Von Karman Facility
ARO, Inc.
Arnold Air Force Sta., Tenn.

Mr. Charles I. Beard
Geo-Astrophysics Lab.
Boeing Sci. Res. Labs.
P. O. Box 3981
Seattle, Washington 98124

Mr. Jay Fox
TRW Systems
One Space Park
Redondo Beach, Calif. 90278

Mr. H. F. Lewis
5 MC Arc Heater Section
LORHO-TRIPLtee Branch
Arnold Research Organization
Ames Div.
Moffett Field, Calif. 94035

Mr. J. D. Rogers
Univ. of Calif.
Los Alamos Sci. Lab.
P. O. Box 1663
Los Alamos, N. M. 87544

Mr. Pat Harney
AFCRL/CRES
Bedford, Mass. 01730

Mr. H. K. Weiekmann
National Physics & Chem. Lab.
Boulder, Colorado 80302

Mr. D. Fultz
Hydrodya Lab.
Univ. of Chicago
Chicago, Ill. 60637

Mr. N. Engler
Univ. of Dayton
Res. Inst.
300 College Park Ave.
Dayton, Ohio

Mr. W. Mermagen
U. S. Army
Ballistic Res. Lab.
Aberdeen Proving Gd., Md. 21005

Mr. F. Badgley
Travelers Res. Center
250 Constitution Plaza
Hartford, Conn. 06103

Mr. G. Warnecke
NASA/GSFC, Code 622
Greenbelt, Md. 20771

Mr. I. Katz
Applied Physics Lab.
Johns Hopkins Univ.
Silver Spring, Md. 21218

Mr. J. Stackpole
NMC Weather Bureau
Washington, D. C. 20546

Mr. J. F. King
GCA Corp.
Bedford, Mass. 01730

Mr. E. R. Walker
Frozen Sci. Res. Group
Dept. of Energy, Mines & Resources
825 Devonshire Road
Esquismalt, B. C., Canada

Dr. Lester Machta, Act. Dir.
Inst. for Atmos. Sci.
Boulder Colorado 80302

EXTERNAL DISTRIBUTION (Continued)

Prof. H. B. Nottage
Univ. of Calif.
Dept. of Engr.
405 Hilgard Ave.
Los Angeles, Calif. 90024

Dr. R. M. White, Adm.
Environmental Sci. Services Adm.
Washington Science Center
Rockville, Md. 20852

National Environ. Satellite Center
Federal Ofc. Bldg. No. 4
Suitland, Md. 20852
Attn: Dr. D. S. Johnson, Dir.
Dr. J. P. Kuettner

Dr. J. H. Leonard, Dir.
Nuclear Sci. & Engr.
Univ. of Cincinnati
Cincinnati, Ohio 45221

Dr. P. S. Kelbanoff
U. S. Dept. of Commerce
National Bureau of Standards
Washington, D. C. 20234

Mr. Wilbur Paulsen
Air Force Cambridge Res. Lab.
L. G. Hanscom Field
Bedford, Mass 01730

E. Summerscales
Mech. Engr. Dept.
Rensselaer Polytechnic Inst.
Troy, N. Y. 12181

Prof. J. R. Weske
Univ. of Md.
College Park, Md. 20746

M. V. Morkovin
1104 Linden Ave.
Oak Park, Ill. 60302

Dr. Lester Lees
Princeton Univ.
Princeton, N. J.

Prof. Stanley Corrsin
Dept. of Mech.
Johns Hopkins Univ.
Charles & 34th St.
Baltimore, Md. 21218

Prof. L. S. G. Kovasznay
Dept. of Mech.
Johns Hopkins Univ.
Charles & 34th St.
Baltimore, Md. 21218

Dr. Carl H. Gibson
Univ. of San Diego
Alcala Park
San Diego, Calif. 92110

Wm. J. Yanta
U. S. Naval Ordnance Lab.
Bldg. 90, Rm. 201G
Silver Springs, Md. 20901

Mr. D. L. Brott
U. S. Naval Ordnance Lab.
Bldg. 90, Rm. 201G
Silver Springs, Md. 20901

Dr. S. Kavipurapu
Dept. of Nuclear Engr.
Univ. of Cincinnati
Cincinnati, Ohio 4522

Langley Res. Center
Hampton, Va. 23365
Attn: S. L. Seaton, MS 235
A. C. Holup, MS 235
Mr. Fedziuk, MS 117
Mr. Boswinkle, MS 117
Mr. Bertram, MS 130
Mr. Hubbard, MS 239
Mr. Runyan, MS 242
Mr. Donely, MS 246

Univ. of Alabama
Res. Inst.
University, Ala. 35486
Attn: Dr. R. Hermann
Dr. Shi

EXTERNAL DISTRIBUTION (Continued)

Smithsonian Inst. Astro. Obs.
Cambridge, Mass.
Attn: Dr. Charles Lundquist

U. S. Army Missile Command
Redstone Arsenal, Alabama
Attn: O. M. Essenwanger, R&D
S. H. Lehnigk, R&D
B. Steverding, R&D

Colorado State Univ.
Ft. Collins, Colorado 80521
Dept. Atmos. Sci.
Attn: E. R. Reiter
W. R. Green
Dr. Baldwin
Mr. Huff
Mr. Simon
Dept. Civil Engr.
V. H. Sandborn
Dept. Math & Statistics
M. M. Siddigui

University of So. Hampton SO9 5NH
South Hampton, England
Attn: Prof. M. J. Fisher
Prof. P. O. A. L. Davies
Inst. of Sound & Vibration Research

Prof. H. Ribner
Univ. of Toronto
Toronto, Canada

Prof. J. E. Ffowcs Williams
Dept. of Math.
Prince Consort Rd. (Exhibition Rd)
Imperial College
London S. W. 7, England

Dr. Kurzweg
Director Res. Div.
NASA Hdqs. Code RR
Washington, D. C. 20546

Dr. B. H. Goethert
Univ. of Tenn. Space Inst.
Tullahoma, Tenn.

Prof. Wallace D. Hayes
Princeton Univ.
Princeton, N. J.

Dr. L. H. Caveney
Ferrestal Campus
Princeton Univ.
Princeton, N. J.

Dr. Ben Zinn
Dept. of Aerospace Engr.
The Georgia Inst. of Tech.
Atlanta, Ga.

Dr. H. Plumblee
Lockheed Georgia Co.
Marietta, Ga.

Dr. P. J. Westernelt
Brown Univ.
Providence, R. I.

Dr. Martin Summerfield
Princeton Univ.
Princeton, N. J.

Dr. Han Liepmann
Calif. Inst. of Tech.
4800 Oak Grove Dr.
Pasadena, Calif. 91103

Dr. Susumu Karaki
1909 Seminole Dr.
Ft. Collins, Colorado 80521

Dr. Helmut Bauer
Dept. of Engr. Sci. & Mech.
The Georgia Inst. of Tech.
North Ave.
Atlanta, Georgia 30332

The Ga. Inst. of Tech.
North Ave.
Atlanta, Ga. 30332
Dept. of Aerospace Engineering
Attn: Dr. A. L. Ducoffe
Dr. R. B. Gray
Mr. J. E. Hubbartt
Dr. J. C. Wu
Dr. A. B. Huang
Dr. B. T. Zinn
Dr. A. C. Bruce

Mr. Richard Wall
Thiokol Chemical Corp.
Redstone Arsenal, Alabama